Available online at www.sciencedirect.com
ScienceDirect
Applied Soft Computing 7 (2007) 286–297
Applied Soft Computing
www.elsevier.com/locate/asoc

Neural network classification of homomorphic segmented heart sounds

Cota Navin Gupta [a,*], Ramaswamy Palaniappan [b], Sundaram Swaminathan [a], Shankar M. Krishnan [a]

[a] *Biomedical Engineering Research Center, Nanyang Technological University, Singapore*
[b] *Department of Computer Science, University of Essex, Colchester, UK*

Received 4 January 2005; received in revised form 2 June 2005; accepted 19 June 2005

Abstract

A novel method for segmentation of heart sounds (HSs) into single cardiac cycle (S_1-Systole-S_2-Diastole) using homomorphic filtering and K-means clustering is presented. Feature vectors were formed after segmentation by using Daubechies-2 wavelet detail coefficients at the second decomposition level. These feature vectors were then used as input to the neural networks. Grow and Learn (GAL) and Multilayer perceptron-Backpropagation (MLP-BP) neural networks were used for classification of three different HSs (Normal, Systolic murmur and Diastolic murmur). It was observed that the classification performance of GAL was similar to MLP-BP. However, the training and testing times of GAL were lower as compared to MLP-BP. The proposed framework could be a potential solution for automatic analysis of HSs that may be implemented in real time for classification of HSs.

Keywords: Grow and Learn neural network; K-means clustering; Multilayer perceptron-Backpropagation neural network; Phonocardiogram signals; Segmentation of heart sounds; Wavelet transform

1. Introduction

Cardiac auscultation is widely used by physicians to evaluate cardiac functions in patients and detect presence of abnormalities. It is however a difficult skill to acquire. Phonocardiography is the recording of sonic vibrations of heart and blood circulation [1]. Because phonocardiography (PCG) can provide valuable information concerning the function of heart valves and the hemodynamics of the heart, it has a high potential for detecting various heart diseases [2]. Nowadays signals produced by the heart are not only heard using a stethoscope but also observed as phonocardiograms on monitor screen. Many pathological conditions that cause murmurs and aberrations of HSs manifest much earlier in phonocardiography than are reflected by symptoms. Thus by proper interpretation of the phonocardiogram (PCG) signal, corrective measures can be taken.

* Corresponding author. Tel.: +65 914 967 23.
E-mail address: cnavin_gupta@pmail.ntu.edu.sg (C.N. Gupta).

1568-4946/$ – see front matter © 2005 Elsevier B.V. All rights reserved.
doi:10.1016/j.asoc.2005.06.006

The heart sound signal or PCG signal of a normal heart is comprised of two distinct activities namely the first heart sound, S_1 and the second heart sound, S_2. These correspond to the normal heart sounds of lup and dup, respectively. In the case of an abnormal heart, there could be several other signal activities between first and second sounds. The extraneous signal activities between S_1 and S_2 are considered as abnormal sound signals (like S_3, S_4, murmurs, clicks and snaps), which are helpful in detecting heart diseases.

There has been a gradual decline in PCG research activity, which might be attributed to the popularity of electrocardiogram (ECG) and also due to the development of various new diagnostic modalities like ultrasound imaging and Doppler techniques. However, these diagnostic tests do not confirm all valvular diseases. Auscultation and phonocardiography not only provide important clinical information but are also simple to use and cost effective. PCG is also an excellent tool for auscultation training and helps in the understanding of the hemodynamics of the heart. In developing countries, where some medical facilities are still considered a luxury, this cost-effective way of providing medical care would improve the life expectancy of patients with valvular pathologies. With advances in digital signal processing, making PCG-based diagnostic techniques available to every doctor would reduce the referral of patients to unaffordable and expensive tests. In most cases, the activities in the PCG signal relating to a given disease are contained in a single interval of cardiac cycle. For implementation of automatic analysis, it is necessary to detect single cardiac cycle, extract features from the single cycle and then classify the signal.

In a previous study [3], each component of S_2 has been modelled by a narrow-band non-linear chirp signal having a fast decreasing instantaneous frequency with time. The two components of S_2 (A_2 and P_2) were defined by a pair of functions, which described the signal envelope and instantaneous phase. The study highlighted the fact that S_2 is a modulated signal. In a different study [4], isolation and extraction of overlapping aortic and pulmonary components were achieved using non-linear chirp signal modelling approach.

Attempts to segment PCG signals have been reported in literature. Many of them depend on ECG signal or/and carotid pulse, as [5]. Correlation techniques were also used in absence of ECG [6]. This method may not perform well when the duration and the spectra of sound signal components show huge variations and this technique cannot be automated. Microprocessor controlled heart sounds gate (HSG), which identifies S_1 and S_2 sounds from PCG alone was reported in [7]. In [8], spectral tracking strategy was used to identify sound signals in the presence of murmurs. Recently, segmentation was achieved using wavelet decomposition and reconstruction into four parts (S_1, S_2, systolic period, diastolic period) [9]. In this method, on selected detailed and approximate signals, a segmentation process was carried out based on envelope calculated from Shannon energy using a continuous time window of 0.02 s with 0.01 s overlap.

Feature vectors are usually obtained from the segmented HSs for classification. In [10], features like duration of second HSs, peak intensity, duration of largest frequency components from the original signal and three selected sub-band signals formed the 95 elements of the feature vector. Daubechies wavelet of sixth order was used to decompose the signal. Coifman fourth-order wavelet was used in [11] to characterize five different heart disease cases. Feature extraction algorithm based on wavelet packet decomposition was proposed in [12].

Classification of various cases of HSs has been studied. MLP-BP has been used to classify HSs in [10] and [13]. Two-dimensional self-organising map were trained using time frequency features of three cases of HSs in [14] but satisfactory performance was not reported. Wavelet based fuzzy neural networks also have been used to detect coronary artery disease in [15].

The goal of this work is to combine segmentation, feature extraction and classification to detect, characterise and interpret HSs. We propose a new method for segmentation of HSs using homomorphic filtering and K-means clustering to segment single cardiac cycle. Each class of HSs contains distinctive information that exists in time and frequency domains. The signal formed by wavelet detail coefficients at the second decomposition level obtained using Daubechies-2 wavelets as in [16] was split into 32 sub-windows that each contains 128 discrete data. The elements of feature vectors were formed by the powers of the signals within these sub-windows. Classifica-

tion was achieved using GAL, similar to previous study [16] and MLP-BP. GAL has advantages of fast training, implementation simplicity, and better performance over MLP-BP [16]. The method proposed in this paper could be developed into a prototype system to aid heart sound analysis.

2. Signal pre-processing

The original signal was first pre-processed before performing segmentation, feature extraction and classification. We tried normalising the signal by setting the variance of the signal to a value of 1.0 but the segmentation results were poor. As such, the original signal was downsampled to 4000 Hz and normalised according to Eq. (1),

$$x_{\text{norm}}(t) = \frac{x_{4000}(t)}{\max(|x_{4000}(t)|)}, \tag{1}$$

where $x_{4000}(t)$ is the downsampled signal. This normalisation was appropriate as the PCG signals in the database did not contain any high amplitude transients. Normal and abnormal HSs have a frequency range of 50–700 Hz. Higher frequencies are not of clinical significance for analysis and diagnosis hence a low pass Chebyshev type I filter with 3-dB cutoff frequency at 750 Hz was used to filter the HSs. After filtering in the forward direction, the filtered sequence was then reversed and run back through the filter to obtain zero phase distortion.

3. Segmentation

The automatic segmentation algorithm was based on Homomorphic filtering and used K-means clustering to indicate single detected cycle. Homomorphic filtering technique resulted in smooth envelope enabling easy peak detection. Peak conditioning was performed to remove peaks, which do not correspond to S_1 and S_2. K-means clustering of the time intervals between peaks was used to indicate the occurrence of single cardiac cycles and also to point to missed cycles. Appreciable S_1 and S_2 amplitudes as compared to murmurs enhanced the performance of this algorithm.

3.1. Peak detection using homomorphic filtering

The approach made use of the similarity in structure of HSs to modulated components. Heart sound signal activities (S_1, S_2) are similar to amplitude modulated waveform while heart murmurs are found to be similar to amplitude and frequency modulated waveform. Homomorphic filtering, which have been used to extract voiced components of the speech [17] was applied to HSs to find the envelope. This is important to find the locations of S_1 and S_2. It provided smooth envelope of the signal with physical meaning and the envelope resolution (smoothness) can be controlled, if desired. Homomorphic filtering technique converts a non-linear combination of signals (multiplied in time domain) into a linear combination by applying logarithmic transformation. Thus, the resulting spectrum can be viewed as a combination of slowly varying and fast varying parts wherein the high frequency content would be removed using a low-pass filter.

Energy of PCG signal was computed and homomorphic filtering gave envelope of the signal, which allowed the peak detection. Homomorphic filtering procedures that we used are as given below:

- Let $v(n)$ represent the PCG signal and $x(n)$ the energy of the PCG signal; then we can express the energy of PCG signal by:

  $$x(n) = a(n)\, f(n), \tag{2}$$

  where $a(n)$ is the slow varying part and $f(n)$ is the fast varying part. S_1 and S_2 contribute predominantly to $a(n)$ while murmurs contribute to $f(n)$;
- To convert multiplication operation to addition, the logarithmic transformation was employed,

  $$z(n) = \log x(n); \tag{3}$$
- Thus

  $$z(n) = \log a(n) + \log f(n); \tag{4}$$

The logarithms of the two signals were now combined in an additive manner. The high frequency component is now characterised by rapid variations in time. We applied the low-pass filter, L to filter the unwanted components.

$$z_l(n) = L[z(n)]; \tag{5}$$

Assuming the logarithmic transformation does not affect the separability of the Fourier components of $a(n)$, $f(n)$ and also since L is linear, we have:

$$z_l(n) = L[\log a(n)] + L[\log f(n)] \approx \log a(n). \quad (6)$$

By exponentiation, we arrived at:

$$\exp[z_l(n)] \approx \exp[\log a(n)] = a(n). \quad (7)$$

After some preliminary experimentation, low pass Chebychev filter (L) was used with transition bandwidth from 10 to 20 Hz. The exponentiation operation enabled us to obtain a smooth envelope of the signal as shown in Figs. 1 and 2, which allowed easy peak detection. Maximum value of the envelope was detected and all points greater than 0.35 of maximum value were considered as peaks. Homomorphic filtering used here involved the retrieval of the envelope i.e. $a(n)$ of the PCG signal and attenuating the contribution from $f(n)$ using L.

The observations made after homomorphic filtering were

- Normal HSs had both slow varying and fast varying parts. S_1 was in low frequency range and a high frequency range [18] with the dominant frequency being between 100 and 200 Hz. The slow varying part was from S_1 and S_2 while the fast varying part was due to the higher frequency component of S_1 (M_1) or S_2 (A_2). Noise also contributed to the envelope in the systolic and diastolic regions but was reduced in amplitude.
- In heart sounds with murmur the fast varying parts in the systolic region (Systolic murmur) and diastolic region (Diastolic murmur) were due to the murmurs.

3.2. Peak conditioning

Peak conditioning was performed for the obtained peaks using homomorphic filtering, which enabled cycle detection process. It involved the rejection of peaks, which did not correspond to the first and second HSs. Parameters of the peaks like peak width, peak start point, peak end point and distance between peaks were found. Steps performed to achieve peak conditioning were:

Step 1. The time between the two detected peaks, which corresponds to time between S_1 and S_2 cannot be less than 80 ms. During inspiration the two components of S_2 (A_2 and P_2) can be separated from each other by 30–80 ms [19]. If this is less than 80 ms, then it corresponds to a split S_2 and the split peaks of S_2 were combined into a single peak.

Step 2. The mean width of detected peaks was calculated and all peaks less than 0.5 of mean peak width were considered as peaks, which do not correspond to S_1 and S_2 and were rejected.

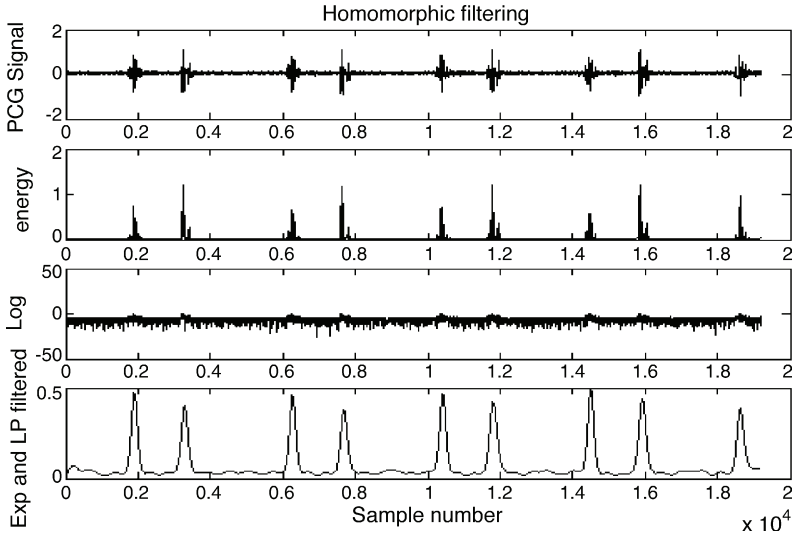

Fig. 1. Peak detection for PCG signal (Normal).

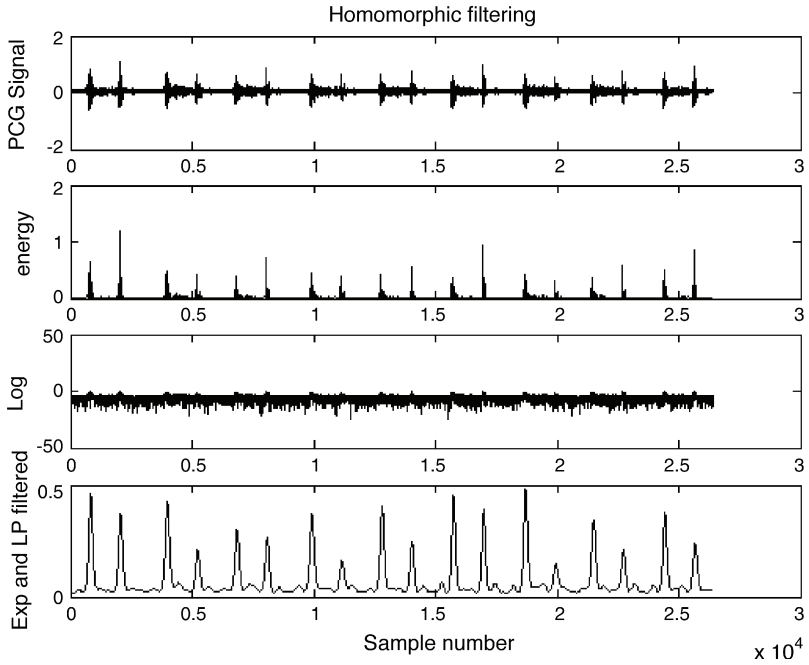

Fig. 2. Peak detection for PCG signal (Systolic murmur).

Step 3. The range of possible width of S_1 and S_2 is 80–120 ms. Greater peak widths, which do not correspond to S_1 and S_2, might result from Step 1 (i.e. when combining split peaks of S_2 into a single peak). These combined peaks might correspond to S_2 sound and murmur like in the case of Diastolic murmur (aortic regurgitation) as shown in Fig. 3. These peaks were limited to 120 ms and peak conditioning was achieved.

Peaks corresponding to only S_1 and S_2 were obtained after peak conditioning as shown in Figs. 4–6 for Diastolic murmur, normal and Systolic murmur, respectively. This enables easy single cardiac cycle detection.

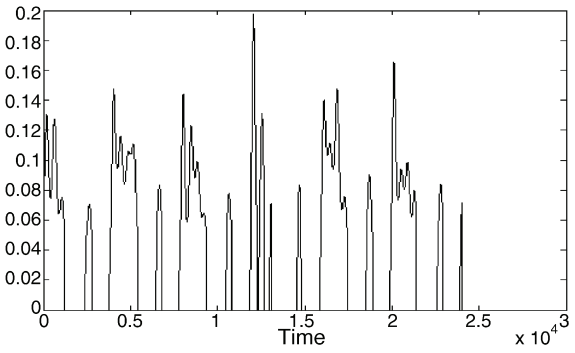

Fig. 3. Combined peaks in PCG signal (Diastolic murmur).

3.3. Cycle detection

This stage involves the extraction of single cardiac cycle of PCG signal after the peak detection and peak conditioning stages. K-means clustering helps to

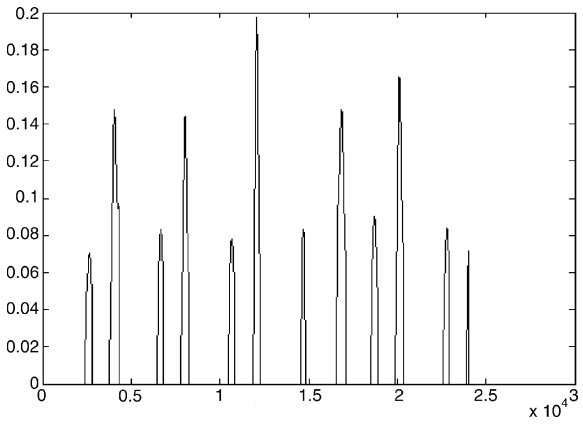

Fig. 4. Combined peaks widths in PCG signal conditioned (Diastolic murmur).

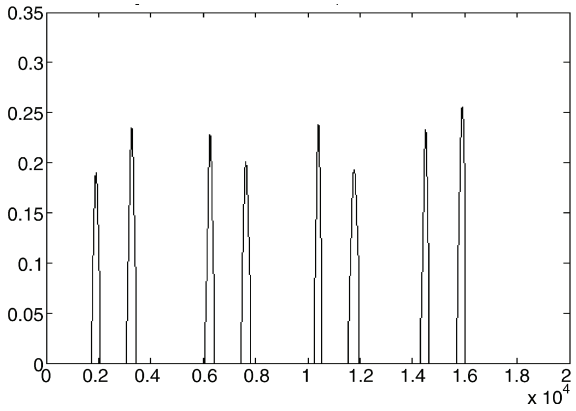

Fig. 5. Peak conditioning of PCG signal (Normal).

indicate single cardiac cycles and is a non-hierarchical partitioning method that partitions the observations in the data into K mutually exclusive clusters, and returns a vector of indices indicating to which of the K clusters it has assigned each observation. It uses an iterative algorithm that minimizes the sum of distances from each object to its cluster centroid, over all clusters. This algorithm moves objects between clusters until the sum cannot be decreased further.

The systolic (S_1–S_2) and the diastolic (S_2–S_1) time intervals excluding the S_1 and S_2 sounds were calculated after the peak conditioning process. The calculated time intervals were clustered into two clusters. The occurrence of cluster 1 and cluster 2 consecutively indicates a single cardiac cycle. The smaller time interval was then identified as systole while the other interval was identified as diastole. Consecutive occurrence of cluster 1 and cluster 1 (or) cluster 2 and cluster 2 might be due to loss of peak, extra peak or due to equal systolic and diastolic intervals. Single cycle of PCG signal was extracted using the clusters as shown in Figs. 7–9 for normal heart sound, heart sound with Systolic murmur and heart sound with Diastolic murmur, respectively.

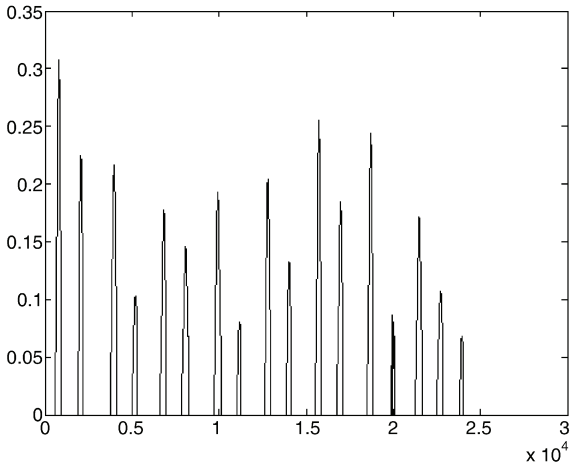

Fig. 6. Peak conditioning of PCG signal (Systolic murmur).

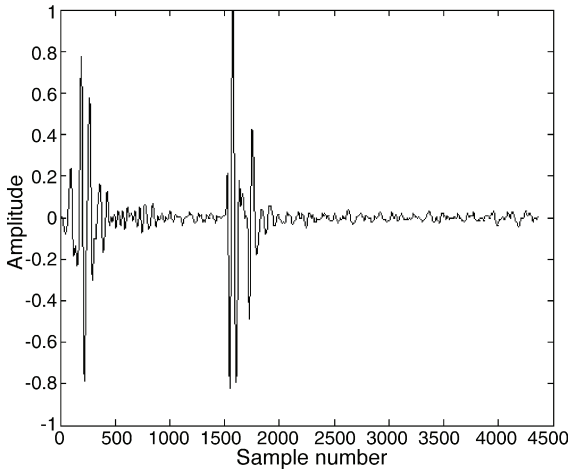

Fig. 7. Single cycle heart sound (Normal).

3.4. Segmentation results

The proposed segmentation algorithm was tested on three classes of HSs (Normal, Systolic murmur and

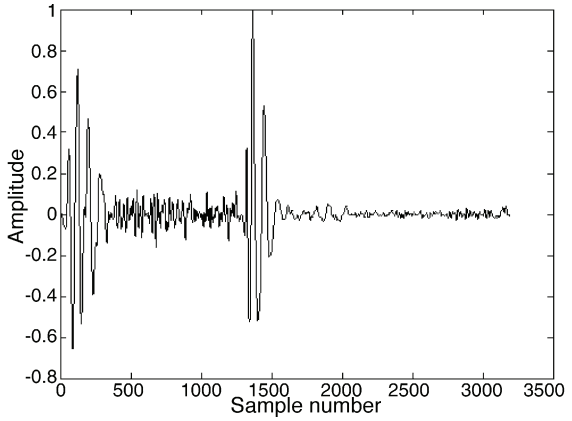

Fig. 8. Single cycle heart sound (Systolic murmur).

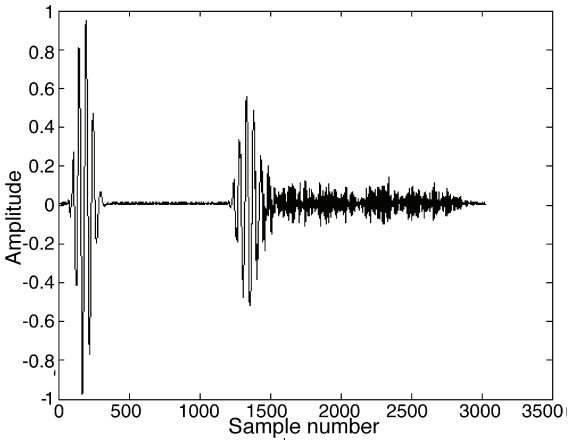

Fig. 9. Single cycle heart sound (Diastolic murmur).

Table 1
Statistics of segmentation algorithm

	Correct	Incorrect	Total	Percentage (%)
Normal	109	1	110	99.09
Systolic murmur	106	18	124	85.47
Diastolic murmur	92	14	106	86.47
Total cycles			340	90.29

Diastolic murmur). The segmentation results are given in Table 1.

High intensity murmurs and high background noise could cause the segmentation algorithm to fail. The incorrectly segmented cycles were hand segmented to enable feature extraction and classification.

4. Feature extraction

Wavelet based feature extraction was applied as in [16] to obtain the features of the segmented PCG signals. PCG signals are non-stationary and the spectrum of the PCG signals were divided into sub-bands to extract the discriminating information from normal and abnormal cases. Discrete wavelet transforms were used for sub-band analysis. The sub-bands for the PCG signal (normal) is shown in Fig. 10. Wavelet coefficients were determined using Daubechies-2 wavelet for the three cases of segmented PCG signals. These coefficients were obtained through a single cycle of PCG signal and wavelet detail coefficients at the second decomposition level were seen to have the distinguishing features as in [16] for three cases of PCG signals. The signal formed by the wavelet detail coefficients at the second decomposition level was split into 32 sub windows with each window containing 128 discrete data values. The elements of the feature vectors were formed by the powers of the signal (32 values) within these sub-windows as in Fig. 11.

5. Classification of heart sounds

Classification of the segmented PCG signal features was achieved using GAL and MLP-BP network. The 32 wavelet features formed the input vector for classification. The 340 segmented heart sounds features were used for the classification algorithms. The performance of GAL as observed in [16,20] has advantages of fast training and better performance over MLP-BP.

GAL algorithm can be used to learn categories in an incremental manner [21]. Class definitions are extended if need arises [21]. Incremental learning algorithms can modify the network structure by addition or removal of units and links. GAL allows learning at one shot since it is incremental and uses local representation. The network has a dynamic structure; nodes and their connections (weights) are added during learning when necessary [16,20,21]. In the sleep (forgetting) phase, the units that were previously stored but which are no longer necessary due to recent modifications are removed to minimize network complexity. The structure of GAL is shown in Fig. 12 [16].

The procedure for GAL learning and forgetting is as follows [16]:

Step 1. Initially choose a number of vectors randomly from the training set as many as the number of classes. Each vector represents only one class. Initialise each chosen vector as an output node of GAL. Initialise the iteration number to zero value.

Step 2. Increase the iteration number. If the iteration number is equal to the chosen maximum value, terminate the algorithm. Otherwise, go to step 3.

Step 3. Choose one vector denoted by X_i randomly from the training set. Compute the distances between

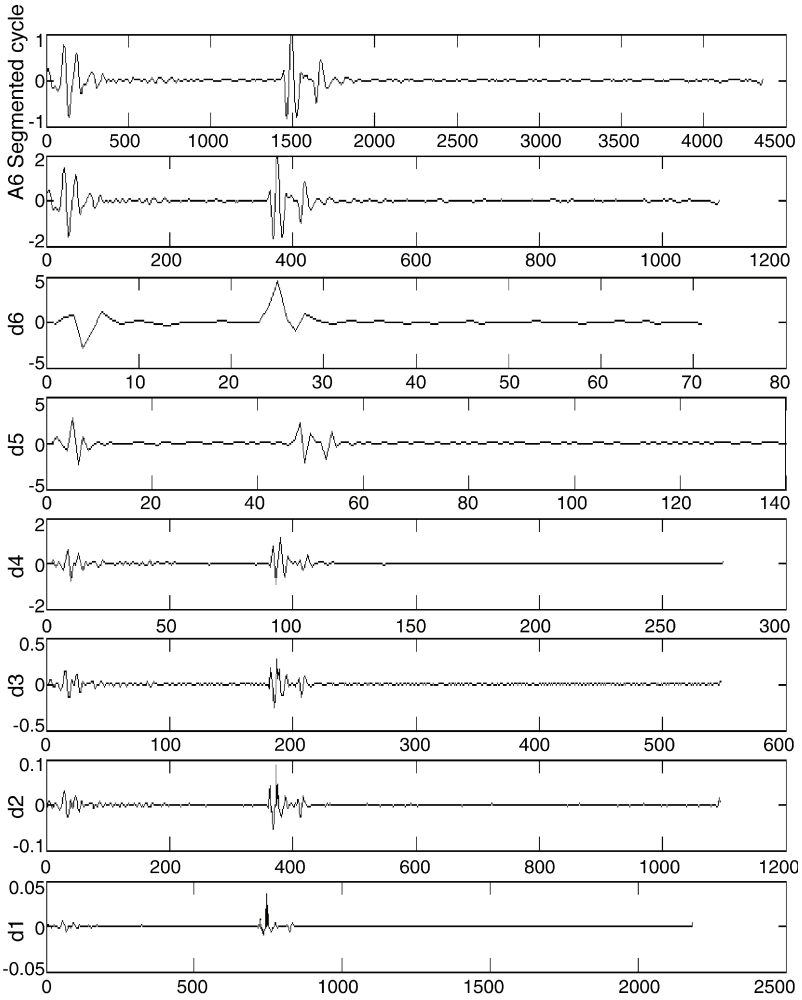

Fig. 10. Wavelet detail coefficients at the first six levels (d^1–d^6) and wavelet approximation coefficient at the sixth level (a^6) for PCG signal (Normal).

each output node of GAL and the input vector, and find the minimum distance as follows:

$$d_o = \sum_{j=1}^{N} (x_j - w_{oj})^2$$
$$d_m = \min_o (d_o) \quad (8)$$

where x_j is the jth element of the input vector X, W_{oj} is the jth element of the oth node of GAL, and N is the number of input nodes. Compare the classes of the input vector and the mth node nearest to the input vector. If their classes are the same, go to Step 2. Otherwise, go to Step 4.

Step 4. Include the input vector in GAL as a new output node. The elements of the input vector are assigned as the associated weights of the new output node of the GAL. Go to Step 2.

During GAL learning, nodes generated depend on the order of the input vectors. A node previously stored may become useless when another node nearer to the class boundary is generated. When a useless node is eliminated from GAL, the classification performance of the network does not change. In order to decrease the network size, these nodes are extracted from GAL by the forgetting algorithm [16] as given below:

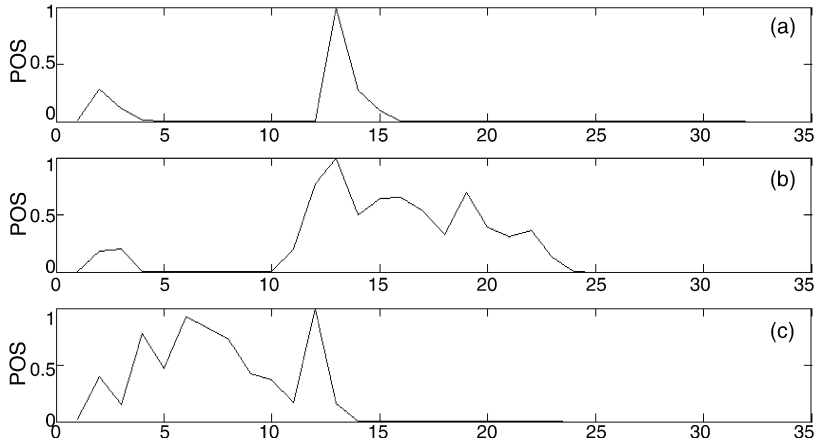

Fig. 11. Feature vector for three cases: (a) Normal, (b) Diastolic murmur and (c) Systolic murmur.

Step 1. Select the maximum iteration number as the number of output nodes in GAL. Initialise the iteration number as zero.

Step 2. Increase the iteration number. If the iteration number is equal to the maximum value, terminate the algorithm. Otherwise, go to Step 3.

Step 3. Choose the next node from GAL in an order. This node is extracted from the network and is given as an input vector to GAL.

Step 4. Compute Eq. (8). Compare the classes of the input vector and the *m*th node of GAL. If their classes are not the same, go to Step 5. Otherwise, go to Step 2.

Step 5. Include the input vector again in GAL. Go to Step 2.

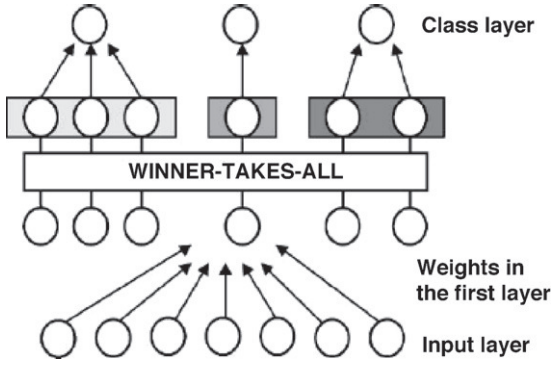

Fig. 12. Structure of GAL.

Classification was also experimented using MLP-BP. Though MLP-BP has been used in recognition of patterns [22] and PCG signal classification [23], it has few drawbacks associated with it. One major problem in MLP-BP is its backpropagation algorithm, which takes long time during learning. The second is associated with the structure wherein the learning rule cannot modify the number of hidden nodes and interconnections. It can modify only the connection weights. Also MLP-BP may get caught in local minima, which might decrease the performance. MLP-BP have at least one hidden layer as shown in Fig. 13.

The Backpropagation algorithm (BP) [24] has served as a useful methodology to train MLP for a wide variety of applications. The BP algorithm is a supervised learning algorithm using feed-forward networks, which makes use of teacher signals or target values. It is basically a gradient descent method and its objective is to minimise the mean squared error between the target values and the actual output of the network. One disadvantage of the algorithm is that in searching for the minimum of the error, it might get stuck in local minima. The BP algorithm basically involves two phases. The first phase is the forward propagation step and the second phase is the backward propagation step. In the forward propagation step, there is no learning and the network will naturally produce an erroneous value at its output before learning. This value is then compared to a target value and the error produced is then back propagated through the layers of the network. This procedure is actually the second phase where learning takes place.

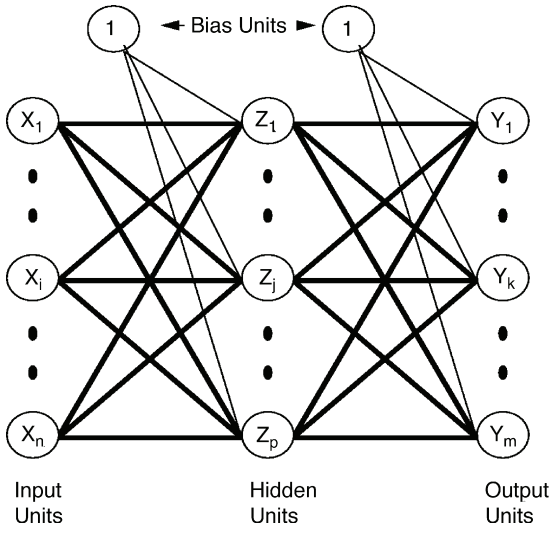

Fig. 13. MLP model with one hidden layer.

The whole process is then iterated over hundreds or even thousands of time depending on the task until the required convergence or when the error limit is reached.

5.1. Classification results

Table 2 shows the performance of GAL for the classification of three cases of HSs (normal: N, Systolic murmur: S, Diastolic murmur: D). The segmented heart sounds dataset (340 patterns) was divided into three datasets each with 112 patterns. Forty-five patterns (15N, 15S, 15D) were used for the training, and 67 patterns (21N, 26S, 20D) were used for testing. Three patterns (1N, 1S, 1D) were used as initial class patterns for the GAL network.

Table 2
Classification using GAL

Performances	Dataset 1	Dataset 2	Dataset 3
Training time	0.1870	0.2660	0.39
Test time	0.0160	0.0170	0.0150
Nodes before forgetting	5	6	3
Nodes after forgetting	4	5	3
Classification of normal	21/21	21/21	21/21
Classification of Systolic murmur	24/26	25/26	24/26
Classification of Diastolic murmur	20/20	20/20	19/20
Classification percentage	97.01	98.50	95.55

Table 3
Classification using MLP-BP

Performances	Dataset 1	Dataset 2	Dataset 3
Training time	2.0630	1.9530	2.035
Test time	0.0940	0.0630	0.0750
Classification of normal	21/21	21/21	20/21
Classification of Systolic murmur	25/26	24/26	25/26
Classification of Diastolic murmur	19/20	20/20	19/20
Classification percentage	97.01	97.01	95.55

Table 3 shows the classification performance of MLP-BP. The input layer consisted of 32 nodes because the number of input features was 32, while the output layer was set to three nodes for the three classes of heart sounds. After some preliminary simulations, we found that 32 hidden nodes gave the best performance. This was also in line with the rule of thumb that says the number of hidden nodes should be set equal to the number of input nodes, which was 32 [25]. The target output for the trained pattern was set to 1.0, while for the rest of the classes, it was set to 0. Training was conducted until the average error fell below 0.01.

6. Conclusion

Information about the health of heart valves is contained in a single cycle of PCG signal. Hence, it is very important to identify single cycle for analysis of defects. Current state of art techniques uses a reference signal like ECG, to obtain a single cycle or to identify the fundamental activities of the PCG signal. We proposed a novel method to segment PCG signal into single cycle using Homomorphic filtering and K-means clustering assuming that the heart rate is uniform for the entire sequence of PCG signal recording. The algorithm has shown a success rate of 90.29%. High intensity murmurs overlapping with S_1 and S_2 could cause the algorithm to fail, though we tried to eliminate this possibility in the peak-conditioning step. Features were obtained using wavelet transform for classification of the various cases of PCG signals. Classification of three classes of HSs was achieved using GAL and MLP-BP neural networks. GAL required less training and testing times

than MLP-BP but with similar performance. It could be used for real-time implementation of HSs classification.

7. Database

With the co-operation of Singapore General Hospital (SGH), 41 volunteers participated in the recording of HSs. The HSs were recorded with 16-bit accuracy and 8000 Hz sampling frequency. No ECG information was used. The various types of PCG signals obtained were N, S and D, which were used to test the algorithms.

Acknowledgements

The authors are grateful to Dr. Sreeraman Rajan (Defense Research and Development, Ottawa, Canada) for his valuable guidance, insightful comments with regards to PCG signals during this work and also for his critical reviews of the above work. We thank Professor Rangaraj M. Rangayyan, Department of Electrical and Computer Engineering, University of Calgary for helping us by providing his PCG papers from old archives. The authors would also like to thank Wang Ping of Biomedical Engineering Research Center, Nanyang Technological University, Singapore for helping us in getting the datasets.

References

[1] E. Vollenhoven, J. Chin, Phonocardiography: past, present and future, Acta Cardiol. 48 (4) (1993) 337–344.
[2] L.G. Durand, P. Pibarot, Digital signal processing of phonocardiogram: review of the most recent advancements, Crit. Rev. Biomed. Eng. 22 (3/4) (1995) 163–219.
[3] X. Jingping, L.G. Durand, P. Pibarot, Nonlinear transient chirp signal modeling of the aortic and pulmonary components of the second heart sound, IEEE Trans. Biomed. Eng. 47 (July (7)) (2000) 1328–1335.
[4] X. Jingping, L.G. Durand, P. Pibarot, Extraction of the aortic and pulmonary components of the second heart sound using a nonlinear transient chirp signal model, IEEE Trans. Biomed. Eng. 48 (March (3)) (2001) 277–283.
[5] R.J. Lehner, R.M. Rangayyan, A three channel microcomputer system for segmentation and characterization of the phonocardiogram, IEEE Trans. Biomed. Eng. 34 (June (6)) (1987) 485–489.
[6] T.S. Leung, P.R. White, W.B. Collis, A.P. Salmon, E. Brown, Time frequency methods for analyzing paediatric heart murmurs, Appl. Signal Process. 4 (3) (1997) 154–167.
[7] M.W. Groch, J.R. Domnanovich, W.D. Erwin, A new heart sounds gating device for medical imaging, IEEE Trans. Biomed. Eng. 39 (March) (1992) 307–310.
[8] A. Iwata, N. Ishii, N. Suzumura, Algorithm for detecting the first and second heart sounds by spectral tracking, Med. Biol. Eng. Comput. 18 (January (1)) (1980) 19–26.
[9] H. Liang, S. Lukkarinen, I. Hartimo, A heart sound segmentation algorithm using wavelet decomposition and reconstruction, in: Proceedings of 19th International IEEE/EMBS Conference, vol. 4, November 1997, pp. 1630–1633.
[10] H. Liang, I. Hartimo, A heart sound feature extraction algorithm based on wavelet decomposition and reconstruction, in: Proceedings of 20th International IEEE/EMBS Conference, vol. 20, no. 3, 1998, pp. 1539–1542.
[11] T.R. Reed, N.E. Reed, P. Fritzson, Heart sound analysis for symptom detection and computer aided diagnosis, Simulation Model. Pract. Theory 12 (May) (2004) 129–146.
[12] H. Liang, I. Hartimo, A feature extraction algorithm based on wavelet packet decomposition for heart sound signals, in: Proceedings of IEEE-SP International Symposium on Time Frequency and Time Scale Analysis, October 1998, pp. 93–96.
[13] D. Barschdorff, S. Ester, E. Most, Phonocardiogram analysis of congenital and acquired heart diseases using artificial neural networks, in: Advances in Fuzzy Systems-Applications and Theory, vol. 3: Comparative Approaches to Medical Reasoning, World Scientific Publishing Co., 1995, pp. 271–288.
[14] T.S. Leung, P.R. White, W.B. Collis, E. Brown, A.P. Salmon, Characterisation of paediatric heart murmurs using self organizing map, in: Proceedings of 21st Annual International Conference of IEEE-EMBS, vol. 2, October 1999, p. 926.
[15] Y.M. Akay, M. Akay, W. Welkowitz, J. Kostis, Non-invasive detection of coronary artery disease, IEEE Eng. Med. Biol. Mag. 13 (November) (1994) 761–764.
[16] T. Olmez, Z. Dokur, Classification of heart sounds using an artificial neural network, Pattern Recognit. Lett. 24 (January) (2003) 617–629.
[17] J.R. Deller, J.G. Proakis, J.L. Hansen, Discrete Time Processing of Speech Signals, Prentice Hall, 1993.
[18] A.P. Yoganathan, R. Gupta, F.E. Udwalia, J.W. Miller, W.H. Corcoran, R. Sarma, J.L. Johnson, R.J. Bing, Use of fast Fourier transform in the frequency analysis of the first heart sound in normal man, Med. Biol. Eng. Comput. 14 (1976) 69–73.
[19] J.A. Shaver, R. Salerni, P.S. Reddy, Normal and abnormal heart sounds in cardiac diagnosis Part I: systolic sounds, Curr. Problems Cardiol. 10 (1985) 2–68.
[20] E. Alpaydin, Neural models of incremental supervised and unsupervised learning, Ph.D. Thesis, Ecole Polytechnique De Lausannne, Switzerland.
[21] E. Alpaydin, GAL: networks that grow when they learn and shrink when they forget, Int. J. Pattern Recognit. Artif. Intell. 8 (1994) 391–414.

[22] A.S. Miller, B.H. Blott, T.K. Hames, Review of neural network applications in medical imaging and signal processing, Med. Biol. Eng. Comput. 30 (1994) 449–464.
[23] D. Barschdorff, D. Ester, S. Most, Phonocardiogram analysis of congenital and acquired heart diseases using artificial neural network, in: Advances in Fuzzy Systems-Applications and Theory (3), Comparative approaches to medical reasoning,, World Scientific Publishing Co., 1993, pp. 271–288.
[24] D.E. Rumelhart, G.E. Hinton, R.J. Williams, Learning representations by back-propagating error, Nature 323 (1986) 533–536.
[25] S. Haykin, Neural Networks: A Comprehensive Foundation, second ed., Prentice Hall, 1999.